Centrum Rzeczoznawstwa Budowlanego

Inżynieria Bezpieczeństwa Obiektów Antropogenicznych 4 (2022) 12-41
https://inzynieriabezpieczenstwa.com.pl/

Inżynieria Bezpieczeństwa Obiektów Antropogenicznych

Experimental and theoretical study of the reinforced concrete flat slabs with the central support loss

Viktar TUR[*1], Andrei TUR[2], Aliaksandr LIZAHUB[3]

[1] Dr. Sc., Professor, Head the Department of Concrete Technology and Construction Materials, Brest State Technical University, Belarus
Professor, Dr. Sc., Professor of the Department of Building Structures, Bialystok University of Technology, Poland

[2] PhD, Associate Professor, Head the Department of Architecture, Brest State Technical University, Belarus

[3] Master of eng. science, junior research fellow, Department of Building Structures, Brest State Technical University, Belarus

Abstract

The paper experimentally and theoretically considers the issues of assessing the robustness and resistance to progressive collapse of a flat slab with a sudden removal of the central support.

The results of testing two scale models of a fragment of a flat ceiling in the case of removal of the central support under static (specimen FS-1) and dynamic (specimen FS-2) loading are presented and analyzed.

A theoretical approach to the quantitative assessment of robustness was tested, which is based on the provisions of the energy balance of a damaged structural system in an accidental design situation.

Keywords: flat slab, robustness, resistance mechanism, membrane action, dynamic resistance, energy balance method.

Introduction

The problem of the progressive collapse prevention of newly designed and existing structural systems, which originates from the accident of the Ronan Point residential building (1968, England), does not lose its relevance, but also acquires new significance due to the increased level of risks to which humanity is exposed. Therefore, the progressive collapse of the reinforce concrete (RC) structural systems has risen much attention among the engineering community due to the frequent occurrence of accidental hazardous around the world, caused substantial loss of life and properties [4, 8, 17, 19, 30].

As was shown in [8] the multi-story RC building with flat slabs are one of the widely-used structural system in engineering practice. According to [4] the number of stories and seismic design intensity had significant effects on progressive collapse resistance of multi-story RC structural systems. It was found [4] "*that the structure with a higher seismic design intensity had a greater capacity to prevent progressive collapse"*. Moreover, published literature [8,

* **Corresponding author:** E-mail address: (profturvic@gmail.com) Viktar TUR

https://dx.doi.org/10.37105/iboa.156
Received 15 December 2022
Available online 31 December 2022
ISSN 2450-1859, eISSN 2450-8721
Published by Centrum Rzeczoznawstwa Budowlanego

19, 30] point out that the dynamic effects should be included in the robustness assessment since progressive collapse was a typical dynamic event arising from local damage.

Structural system robustness check is performed using non-linear static (NLS) or dynamic (NLD) models that take into account the spatial work of the structural system. It should be noted that although nonlinear dynamics (NLD) transient analyses can provide accurate predictions of structural responses under column removal scenarios, the related modeling is more complicated, and the computational consumption is more demanding compared to the nonlinear static (NLS) analyses [19]. Moreover, nonlinear dynamics procedure consists of sufficient uncertainties and the required computational resources will further increase if all typical column removal scenarios in building need to be evaluated [19]. As was shown in [37], it is thus necessary to develop a simplified and accurate methods to assist in the quick assessment of the progressive collapse fragility of RC structural systems considering the dynamic effects.

Current provisions [2, 3, 7, 9, 13, 33, 34] regulate that the structural systems should be evaluated under systematical alternate path (AP) analyses that comprehensively consider various column removal scenarios. Most structural codes [2, 3, 7, 9, 13, 33, 34] and current studies [8, 17, 19, 30, 37] commonly considered the removal scenarios of one specific column or some of the typical columns (i.e. corner column, edge column and internal column) usually on the ground story of building.

In most cases, the robustness of structural systems is checked by indirect methods, such as the tie force method, aimed at a general increase in the plasticity (ductility) and integrity of structural systems. However, as it was shown in [1, 36, 37], such methods are based on pre-accepted, constant values of limit deflections and do not take into account the real deformability of the tie elements. In some cases a such simplification can lead to an inadequate assessment of the design resistance and overestimation of the robustness of the damaged system. It is assumed that horizontal and vertical tie elements, designed by the method of tie forces [2, 3, 7, 9, 13, 33, 34], in most cases positively affect the robustness of the building as a whole. These effects, in turn, cannot be quantified within the framework of this method.

As was shown above the most dangerous local damage for a structural system is the failure of one specific or some of the typical vertical load-bearing structural elements (for example, a column or a section of a wall). These elements are commonly referred to as key elements. The key element removal scenario leads to the redistribution of the effects caused by the quasi-permanent combination of the gravitational loads applied to the elements of the damaged structural system. If the remain structural elements of the damaged system are able to resist additional effects and effectively redistribute internal forces to adjacent load-bearing elements, then the development of collapse process stops, and the damaged structural system becomes stable. In the opposite case, disproportionate collapse of the damaged structural system occurs.

The known direct methods for robustness assessment (the method of alternative load paths, the method of key elements designing) [8] make it possible to quantify the robustness of a damaged structural system, if the some specific criterion for robustness evaluation are available. However, there is still no generally accepted criterion for assessing robustness in regulatory documents. The most promising is the method of alternative load paths, which involves the sudden removal of a key element from the system and further analysis of the resistance of a damaged system (the term "modified system" is often found in the published literature).

The development of the construction industry, the introduction of new materials, the complexity of the applied structural systems on the one hand and the increase in the list of threats (accidental events) that can lead to progressive collapse, on the other, led to the need for theoretical and experimental studies of the robustness of structures in accidental situations and the development of a generally accepted criterion for assessing robustness.

To quantitatively include the dynamic effects in the load effects calculation subject to progressive collapse, an energy-based method was proposed to calculate the dynamic load increase factor by Izzuddin et al [19]. It should be noted that the main idea was that *"the external work of the unbalanced loads caused by the sudden column loss could be dissipated by structure if it did not collapse"* [19].

The quantitative criterion for robustness assessment can be found with usage energy-based method as the ultimate dynamic response of the structural system at the first half-cycle of oscillations after sudden removal of vertical load-

bearing element [19, 37]. In accordance with the energy-based method a complete nonlinear quasi-static response of the damaged structural system is required for calculation of this response.

In the presented paper the multi-story buildings with the flat reinforced concrete floors are considered. Such type of floor (with flat slabs) are widely used in residential, office, administrative and industrial buildings for which economic losses and the threat to people's lives caused by an accidental event can be significant.

Over the past decade, a number of authors have conducted extensive studies in the field of prevention of the progressive collapse of reinforced concrete structural systems [1, 5, 6, 8, 15, 19, 21, 26, 31, 38], including structural systems with flat slabs [22, 25, 28, 29, 32, 39].

Based on results of an available experimental studies [22, 25, 28, 29, 32, 39], it is possible to describe the general case of behavior of a flat slab after the removal of the central support by the relationship "*q*-*δ*" which relates uniformly distributed load and deflection in the central node (see Figure 1).

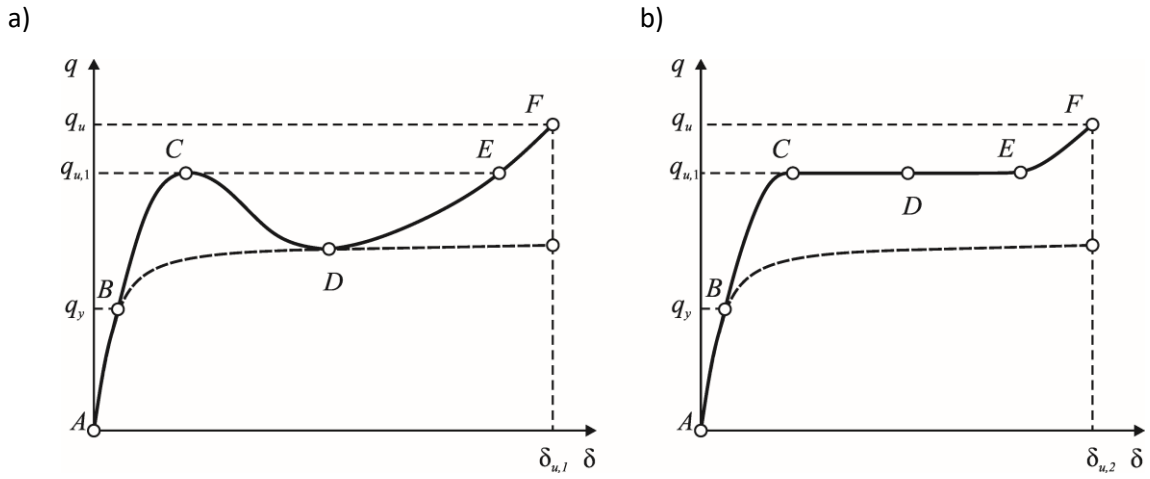

Figure 1. Quasi-static load-displacement diagrams for a flat slab with removal of the central support: (a) loading case with displacement control; (b) loading case with the load control

It should be noted that the "*q*-*δ*" relationship for loading case with displacement control (hard mode, see Figure 1a) and loading case with the load control (soft mode, see Figure 1b) are different. However, according to the energy conservation law, the deformation energy of the system (the area under the "load-displacement" curve, see Figure 1) will be the same for both cases.

In loading case with displacement control as the deflections increase under increased uniformly distributed load (Figure 1a), several characteristic stages can be distinguished in the behavior of the slab, which correspond to the specific resistance mechanisms.

Initially, as the load increases, the deflection increases almost linearly (from point A to point C). Yield lines form and develop in the element (point B) until the maximum resistance is reached (point C). The initial interval A-C of the load-displacement relationship is defined as the elastic or elastic-plastic stage. Some researchers [25] also define this interval as the "stage of a compressed membrane", since compressive forces arise in the plane of the slab with small deflections and restraint of longitudinal deformations. As the result of the interaction of bending moments and longitudinal compressive forces the bending resistance of the flat slab increases. Therefore, the first peak load qu,1 at point C in Figure 1a, will be situated higher than the load corresponding to the yielding point of steel reinforcement qy (point B) obtained from the yield line theory. Deflection at point C for laterally restrained slabs is approximately equal to half the thickness of the slab.

At point C, the slab is completely divided into rigid blocks by yield lines (linear plastic hinges) and transforms to mechanism. The resistance of the slab decreases due to the decrease in compressive membrane forces until the complete destruction of the concrete along the yield lines over the entire height of the slab occurs (point D)

The interval from C to D is defined as transitional. As the load-bearing capacity decreases with increasing deflections and is close to point D, the compressive membrane forces in the slab decrease and turn into tensile ones.

After the point D, the effect of a tension membrane develops. The destruction of concrete occurs in the central region of the span over the entire height of the slab. At this stage whole tensile forces are redistributed to the remain steel reinforcement and/or ties. The failure of the slab occurs at point E and is associated with the failure of the tensile reinforcement and/or ties.

In flat slabs in which additional ties are provided to resist membrane effects, the load at point D may exceed the load at point C [25].

In loading case with the load control (Figure 1b), the response of the structural system immediately falls from point C to point E, in which the membrane resistance effect triggered. This is accompanied by a sudden increase in deflections and, as a consequence, by the appearance of dynamic inertial effects.

Experimental studies [22, 25, 28, 29, 32, 39] show that flat slabs designed in the traditional way (with reliability parameters obtained based on economical optimization procedure according to ISO 2394 [18]) are not able to resist the gravitational loads with accounting the dynamic effects acting on the damaged system after the remove of the key element due to the bending resistance mechanism only or due to the effect of a tensile membrane only.

A number of authors [22, 28, 29, 32, 39] for checking of robustness of the flat slabs try to consider a such mechanisms as the bending, the shear (punching) resistance, the effects of a compressed and tensile membrane together in one design model. However, due to the complexity of modeling the common influence and correlation of all resistance mechanisms, simplified models of structural systems with flat slabs are proposed, which often take into account only one specific resistance mechanism.

The working hypothesis *is that an important role for the robustness of buildings with flat slabs is played by secondary resistance mechanisms that arise and develop during failure, as well as their common action and correlation (influence on each other).*

The main purpose of the presented experimental studies is to investigate the failure mode of flat slabs and to validate proposed theoretical design model applied to assess their robustness after a sudden loss of the central column. To achieve this goal the following tasks were solved:

- design and construction of a scale model of a monolithic reinforced concrete floor with flat slab;
- experimental investigation of the failure mode of the flat slab after sudden removing the central column (under quasi-static and dynamic applied load);
- measurement of the reaction in the removed central support, vertical and horizontal displacements, strains in the tie elements, strains in concrete during step-by-step static and sudden dynamic loading of FS-1 and FS-2 specimen, respectively;
- analysis of experimental data and comparison with theoretical results of calculation with usage proposed model.

1 Experimental study methodology

1.1 Rationale of the test setup design

It should be noted that a number of problems arise associated with the experimental studies of the robustness with usage of the full-scale models. These include material costs, special equipment and test space. Therefore, experimental studies of robustness of the RC flat slabs in the case of a sudden removal of the central column were carried out on scale models.

The experimental program included two cases of vertical loading which modeled the column loss (Figure 2): quasi-static (specimen FS-1) and dynamic (specimen FS-2).

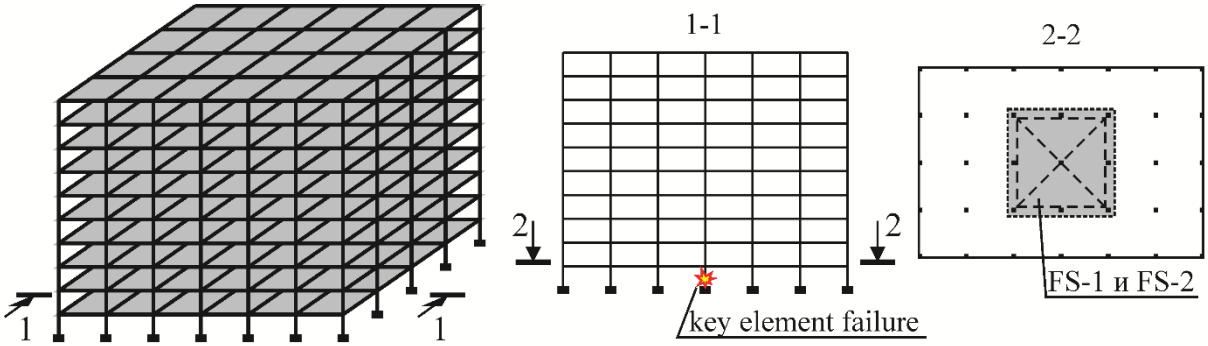

Figure 2. Case of removal of the central column

The prototype of the flat floor was designed in accordance with the requirements of the current code [33, 34]. The scale models were constructed taking into account the scale coefficients of dimension theory and scaling rules [27]. The geometric scale factor was assumed to be $s_L = 6$, and the stress scale factor $s_f = 1$.

Some assumptions were made when modelling the boundary conditions of a flat slab to simplify experimental studies. The columns were modelled using steel plates on which the slab was supported, and the influence of adjacent spans on the horizontal and vertical boundary conditions of the fragment was modelled using contour beams embedded in a rigid steel concrete frame (see Figure 3). These assumptions do not affect the confirmation of the proposed hypothesis.

In the middle of each face along the contour of the slabs, permanent (non-removable) supports C1-C4 were placed. A removable support C5 (C5') was placed in the center of the slab span. In the quasi-static test (specimen FS-1), the central support was modeled by a hydraulic jack. In the dynamic test (specimen FS-2), the central support was a special suddenly removable composite support.

It was shown in a number of publications [26, 32, 39] that at the time of a sudden loss of a column, on the floor, which is situated above the removed key element, act uniformly distributed gravitational loads (combination of self-weight and the long-term component of imposed loads). In experimental studies, the gravitational uniformly distributed load applied on the flat slab was modelled using piece calibrated steel blocks.

1.2 Test specimens description

Each specimen was a scale model of a 2 × 2 span flat slab fragment. All slabs were 2000 × 2000 mm (without contour beams) and 45 mm in height (see Figure 3a). The concrete slabs were reinforced with orthogonal fabric mesh of 2 mm diameter plain wires at 50 mm spacing (62.8 mm2/m) see Figure 3b. The zones under column were reinforced orthogonally with 2 mm wires at 50 mm spacing each direction as illustrated in Figure 3b. The concrete cover for the bottom and top reinforcement meshes was 7 mm. According to the method of tie forces, three reinforcing bars with a diameter of 4 mm are provided as horizontal ties in the middle column strip in two directions of the slab. Tie bars are placed in the middle of the height of the slab section and anchored in the contour beams. The construction and detailing of the test specimens are shown in Figure 3.

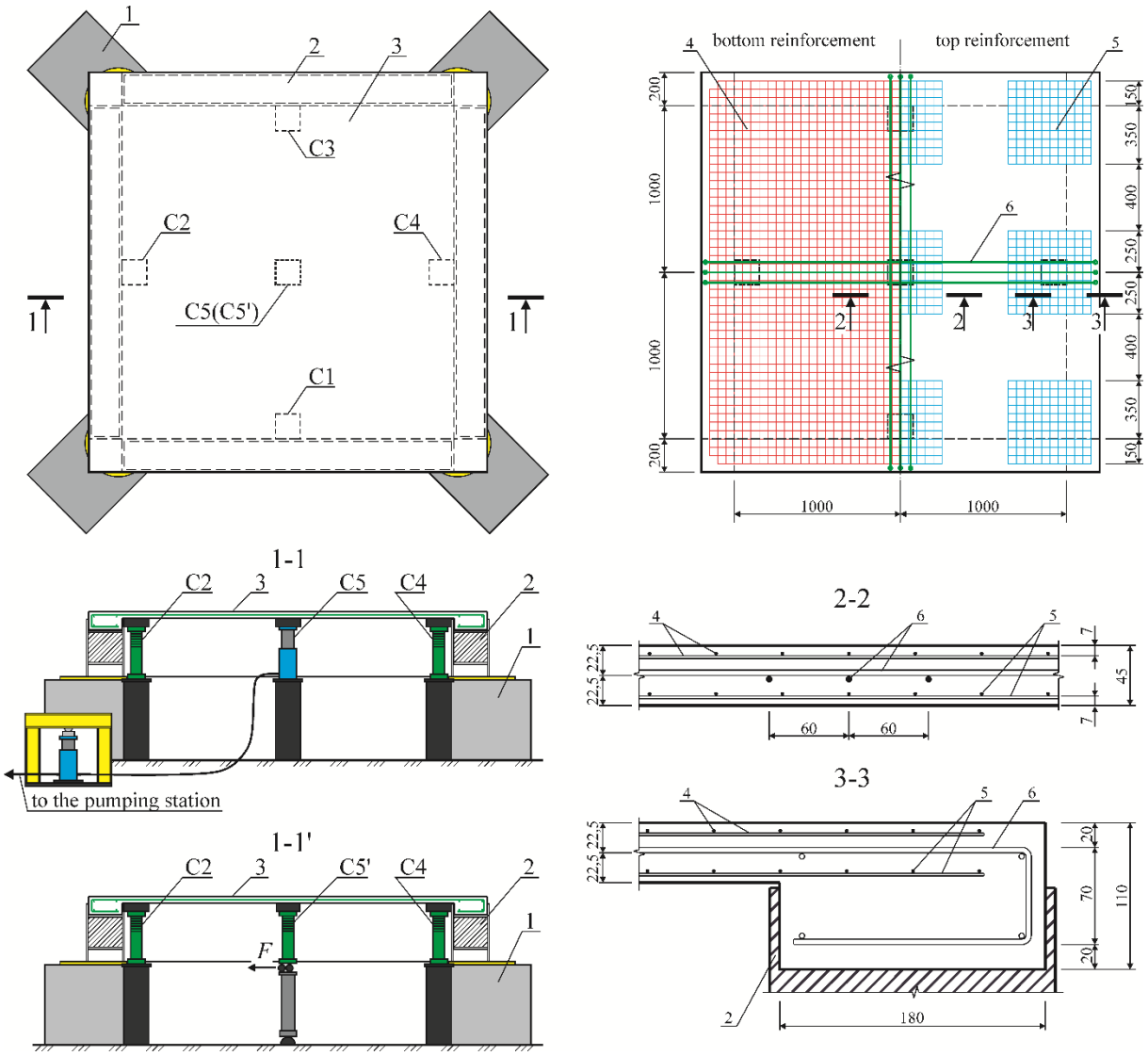

C1..C4 – permanent (non-removable) supports; C5 (C5') – internal removable support; 1 – RC supports for the contour frame; 2 – rigid steel concrete contour frame; 3 – specimen; 4 – top reinforcement made of wire Ø2 with a step of 50×50 mm; 5 – bottom reinforcement made of wire Ø2 with a step of 50×50 mm;

6 – ties (reinforcing bars Ø4)

Figure 3. Design of specimens FS-1 and FS-2: a) general top view, section 1-1 for FS-1, section 1-1' for FS-2; b) scheme of reinforcement of specimens

1.3 Materials, preparation and curing of specimens

The concrete mixture composition was designed taking into account the scale factors and the concreting of the slab in the laboratory conditions. The maximum size of a coarse aggregate was 5 mm. Concrete mix nominal composition per 1 m^3: cement – 520 kg; fine aggregate – 850 kg; coarse aggregate – 900 kg; water – 200 l; Stachement 2010 – 8.2 kg.

The concrete strength was determined from test of the standard cylindrical (150 × 300 mm) and 100×100×100 mm cube specimens. The control specimens were cured in the same conditions as the slabs and tested according to standard methods [14] on the day of testing of each flat slab fragment. The specimens were tested to failure under uniform axial compression load in the Compression Testing Machine of capacity 3000 kN and the loading rate was kept constant for all specimens at 0,15 MPa/sec.

The modulus of elasticity of concrete was determined from test of the standard cylinders (150 × 300 mm) according to the standard procedure [16]. The main mechanical properties of concrete are given in Table 1.

Table 1. Mechanical properties of concrete

Specimen	Average compressive strength, MPa		Average tensile strength, MPa	Modulus of elasticity, GPa	Strains(1) $\varepsilon_c \times 10^3$	
	$f'_{c,cube}$	f_{cyl}	f_{ct}	E_{cm}	peak ε_{c1}	ultimate ε_{cu}
FS-1	73,2	57,34	4,06	32,4	2,46	3,50
FS-2	77,1	65,34	4,57	32,7	2,56	3,11
Note: (1) – Strains at the parametric points of the "stress-strain" relationship are determined in accordance with [34].						

The main mechanical properties of the steel reinforcement in flat slab fragments, are listed in Table 2.

Table 2. Main mechanical properties of the steel wire and reinforcing bars

Diameter Ø, mm	A_s, mm^2	Loading speed, MPa/s	Yield strength f_{ym}, MPa	ε_{sy}, ‰	Tensile strength f_{um}, MPa	ε_{su}(1), %	E_s, GPa
2	3,14	5	306,9	1,53	386,8	18,8	200
4	12,57	10	594,3	2,97	696,8	7,7	200
Note: (1) – Strains at the parametric points of the deformation diagram are determined by testing in accordance with [15].							

Samples of FS-1 and FS-2 slabs were cured under plastic film in laboratory conditions.

1.4 Characteristics of measurement devices

When testing the FS-1 spacemen, vertical and horizontal displacements were measured using deal indicator with a sensitivity of 0.01 mm. To register the vertical deflections of the FS-2 specimen, a special measuring scale with a division price of 5 mm was used together with a laser level and a video camera with a shooting frequency of 60 frames/sec.

The strains of the tie elements in the FS-1 and FS-2 specimen were measured with usage strain gages with a gauge length of 20 mm and an electrical resistance of 100 Ohms. The strain gauge station was two measuring amplifiers "*Spider 8*".

The strain of the concrete of the top face of the FS-1 specimen slab were measured using the extensometer with a gauge length of 300 mm complete with a digital indicator with a sensitivity of 0.001 mm.

During the static unloading test of the FS-1 specimen, a load cell was used to measure the reaction in the central support.

Locations of deflection indicators D1..D7, strain gauges T1..T6 for specimen FS-1 and special measuring scale D1, strain gauges T1, T1'..T6, T6' for the FS-2 specimen are shown in Figure 4. The locations of the extensometer markers S1, S2,...S12 for measuring the concrete strain at the top face of the FS-1 slab are shown in Figure 5.

a) b)

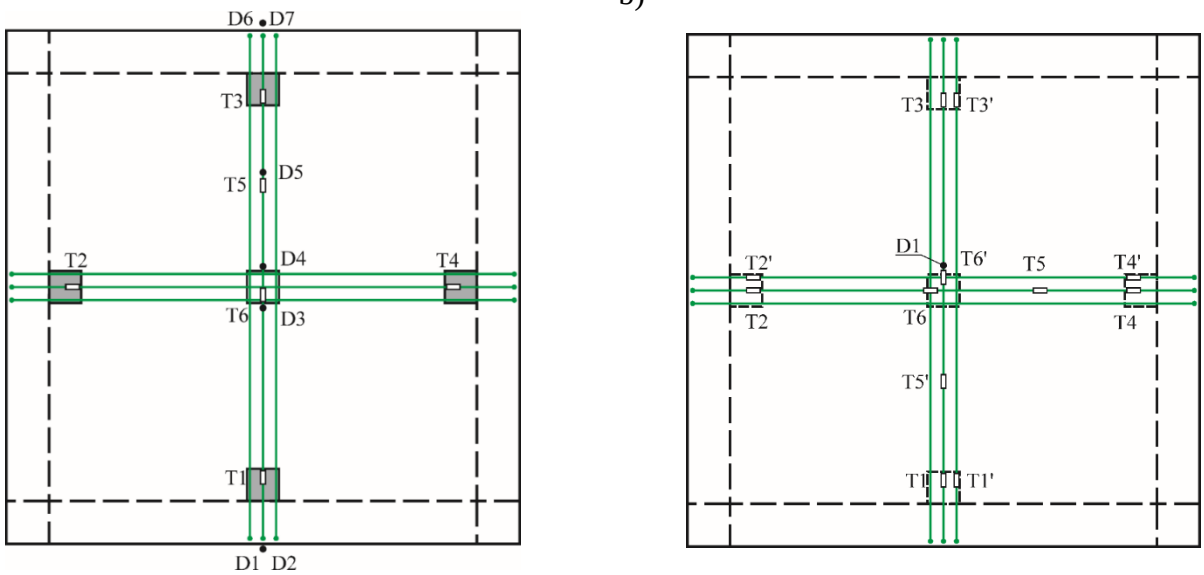

Figure 4. Locations of deflection indicators D1..D7, strain gauges T1..T6 for specimen FS-1 (a) and special measuring scale D1, strain gauges T1, T1'..T6, T6' for the FS-2 specimen (b)

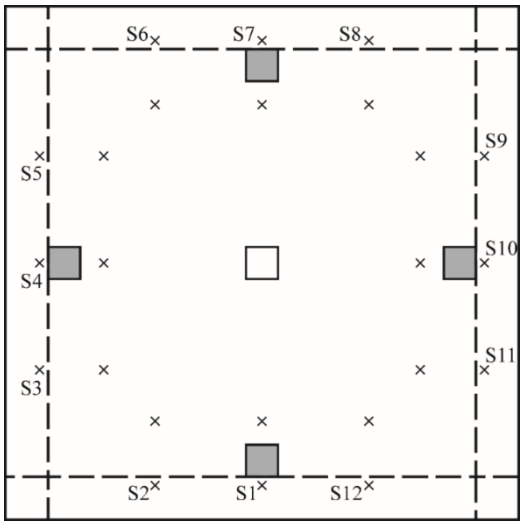

Figure 5. The locations of the extensometer markers S1, S2,...S12 for measuring the concrete strain at the top face of the FS-1 slab

1.5 Testing procedure

The general view of the FS-1 and FS-2 specimens before the tests is shown in Figure 6. Before removing the special suddenly removable composite support the FS-2 specimen was loaded by the uniformly distributed load of the designated level (item 12 Figure 6b).

a)

b)

1 – test specimen; 2 – rigid steel concrete contour frame; 3 – piece calibrated steel weights; 4 – a system of deflection meters for measuring vertical and horizontal displacements; 5 – strain gauge station *Spider-8*; 6 – deformation meter (extensometer) with a base of 300 mm; 7 – load cell (50 kN); 8 – hydraulic jack №2; 9 – rigid steel frame; 10 – pumping station; 11 – central support of sample FS-1 (hydraulic jack №1); 12 – central support of sample FS-2 (composite removable support); 13 – special measuring scale D1

Figure 6. The general view of the FS-1 (a) and FS-2 (b) specimens before the tests

1.5.1 Quasi-static test of specimen FS-1

The FS-1 specimen was tested by the static unloading method proposed in [39]. Although this method does not take into account the dynamic effects of sudden loss of support directly, it allows us to determine the reaction in the removed element at every individual loading stages and to assess the redistribution of internal forces (effects of actions) in the structural system at the global level. It was also emphasized in [26] that testing of the flat slabs by a uniformly distributed load give more realistic results for assessing robustness than testing with concentrated forces applied in the area of the column being removed.

A system consists of two sequentially connected hydraulic jacks and a pumping station was used to measure of the central column reaction (response). The first hydraulic jack acted as a removable central column of the lower

floor and was placed under the test sample. The second jack, together with the load cell, were installed in a rigid steel frame and placed next to the pumping station. The schematic diagram of the jack system at all steps of the loading stage is shown in Figure 7.

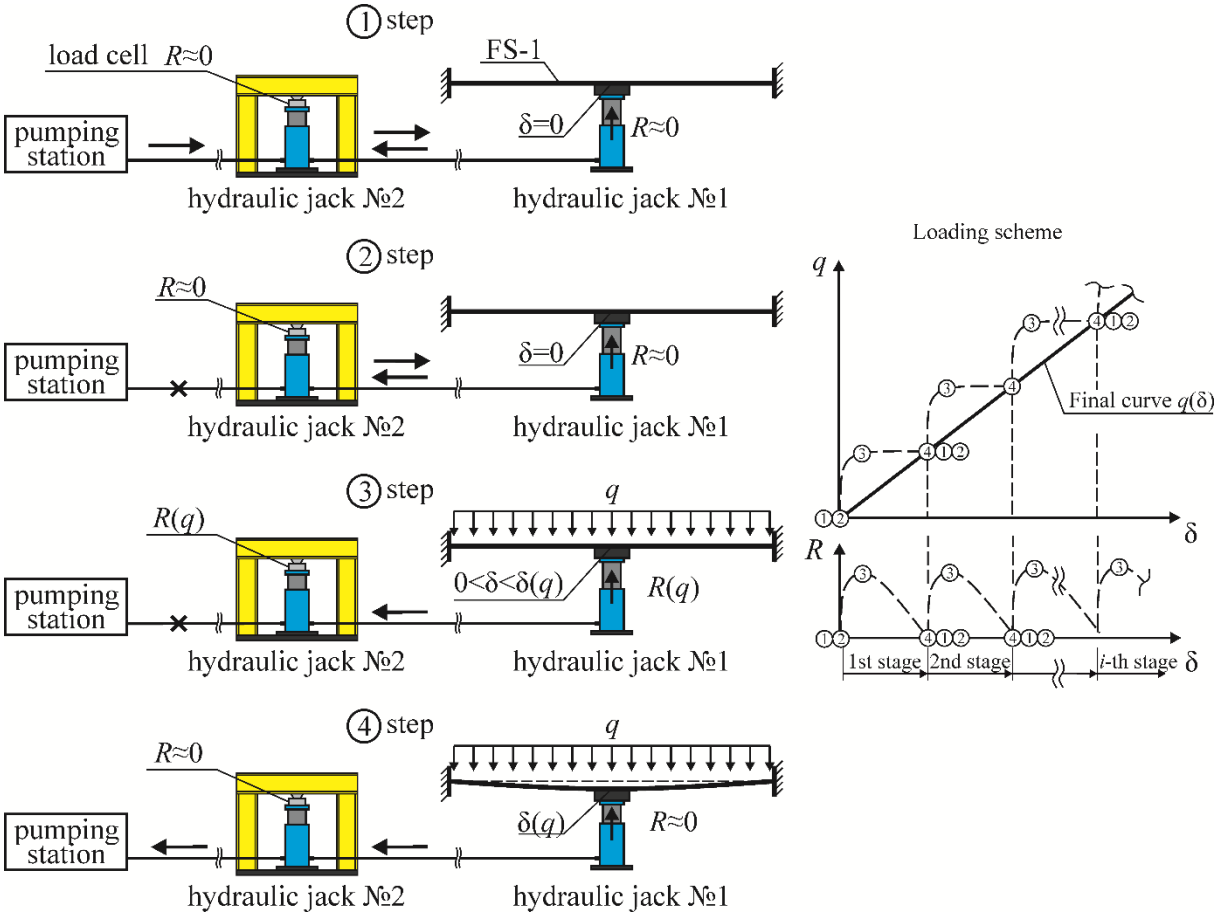

Figure 7. The schematic diagram of the jack system at all steps of the loading stage of FS-1

The uniformly distributed load was modeled by calibrated piece steel blocks.

The reaction in the central support, vertical deflections and strains were recorded at each individual stage of loading as follows:

1) the pumping station applied pressure to the jack system until the jack under the specimen supported the lower face of the slab, which was also reflected on the load cell in the form of a small increment of the reaction R ≈ 0;
2) after that, the valve at the pumping station was closed, which is responsible for pressure relief from the jack system. As a result, at this step, the closed hydraulic system consisting of two jacks was obtained;
3) the sample was loaded with calibrated piece loads, after which the reaction was recorded on the load cell. As a result of loading, the reaction from the loaded slab is transmitted to the first jack, the pressure in the closed system increases and the second jack "compresses" the load cell in a rigid frame. The value of the force registered on the load cell corresponds to the increment of the reaction in the removed support at each individual loading stage;
4) the valve was opened and the pressure from the jack system was smoothly relieved until the reaction on the central support drops to zero (R ≈ 0). After that, vertical deflections and strains of concrete and reinforcement were recorded;
5) then the pressure was applied to the jack system again and all the above steps were repeated again.

1.5.2 Dynamic test of specimen FS-2

The FS-2 prototype was tested under suddenly applied gravitational uniformly distributed load (case of dynamic loading). To simulate the sudden removal of the central column, the special removable support was used (Figure 8).

The uniformly distributed load, as in the FS-1 test, was modeled by calibrated piece weights (calibrated steel blocks).

Dynamic tests of the FS-2 sample included the following steps:

1) installation and centering of a composite removable support;
2) loading of the slab with calibrated steel blocks to the level of the load equal 75% of ultimate quasi-static uniformly distributed load was made. The applied uniformly distributed load value was determined based on the results obtained in quasi-static test of the FS-1 specimen and was equal q = 20.24 kPa;
3) the horizontal force was applied to removable support by the system of cables and blocks as shown in Figure 8. After applying of the horizontal force, the support turns into a mechanism and did not resist the vertical reaction.

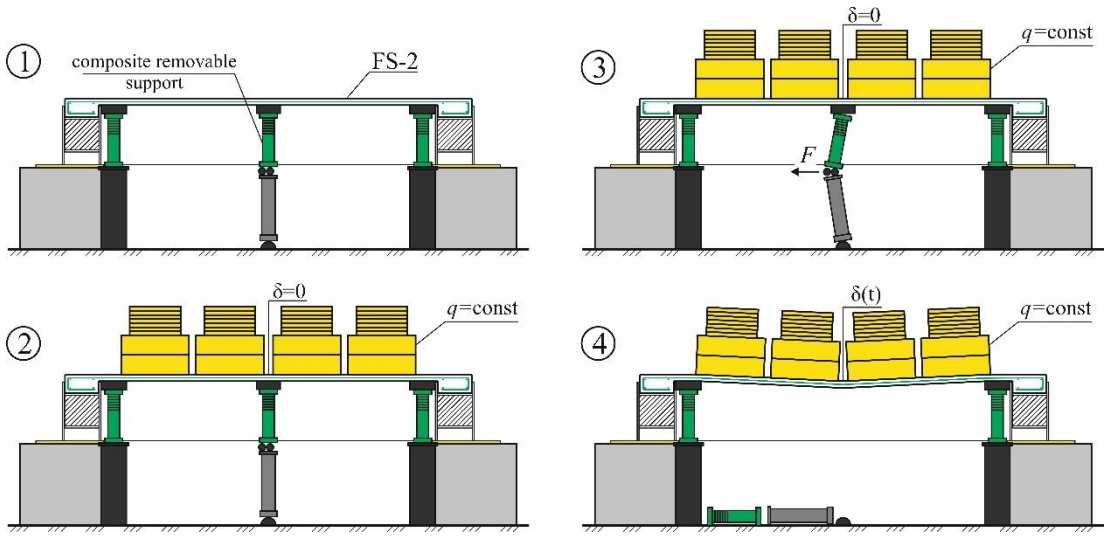

Figure 8. The schematic diagram of the dynamic test of the FS-2 specimen by sudden removal of the central support

2 Results of experimental studies. Analysis and discussion

2.1 Static test of specimen FS-1

In accordance with the methodology outlined in Section 1, the FS-1 sample was tested using the "static unloading" method until complete failure (progressive collapse) of the slab was obtained (Figure 9).

According to the test results, the following data were obtained:

- pattern of crack formation (Figure 9);
- the reaction R in the removable support versus the vertical displacements δ curve and the applied uniformly distributed load q versus vertical displacements δ curve (Figure 10);
- the reaction R in the removable support versus the uniformly distributed load q curve (Figure 11);
- relationship of the concrete strains at the top surface of the slab in span and over column versus the vertical displacements in the central node (Figure 12);

- relationship of the steel ties strains in slab versus the vertical displacements in the central node (Figure 13). It should be noted that at the beginning of the experiment, strain gauges T2 and T5 failed and did not register the change in strains.

As can be seen from Figure 9, the cracks pattern has a slightly asymmetrical character. This can be explained by the initial imperfections of the specimen, as well as the imperfection of the method of loading with piece loads (steel blocks).

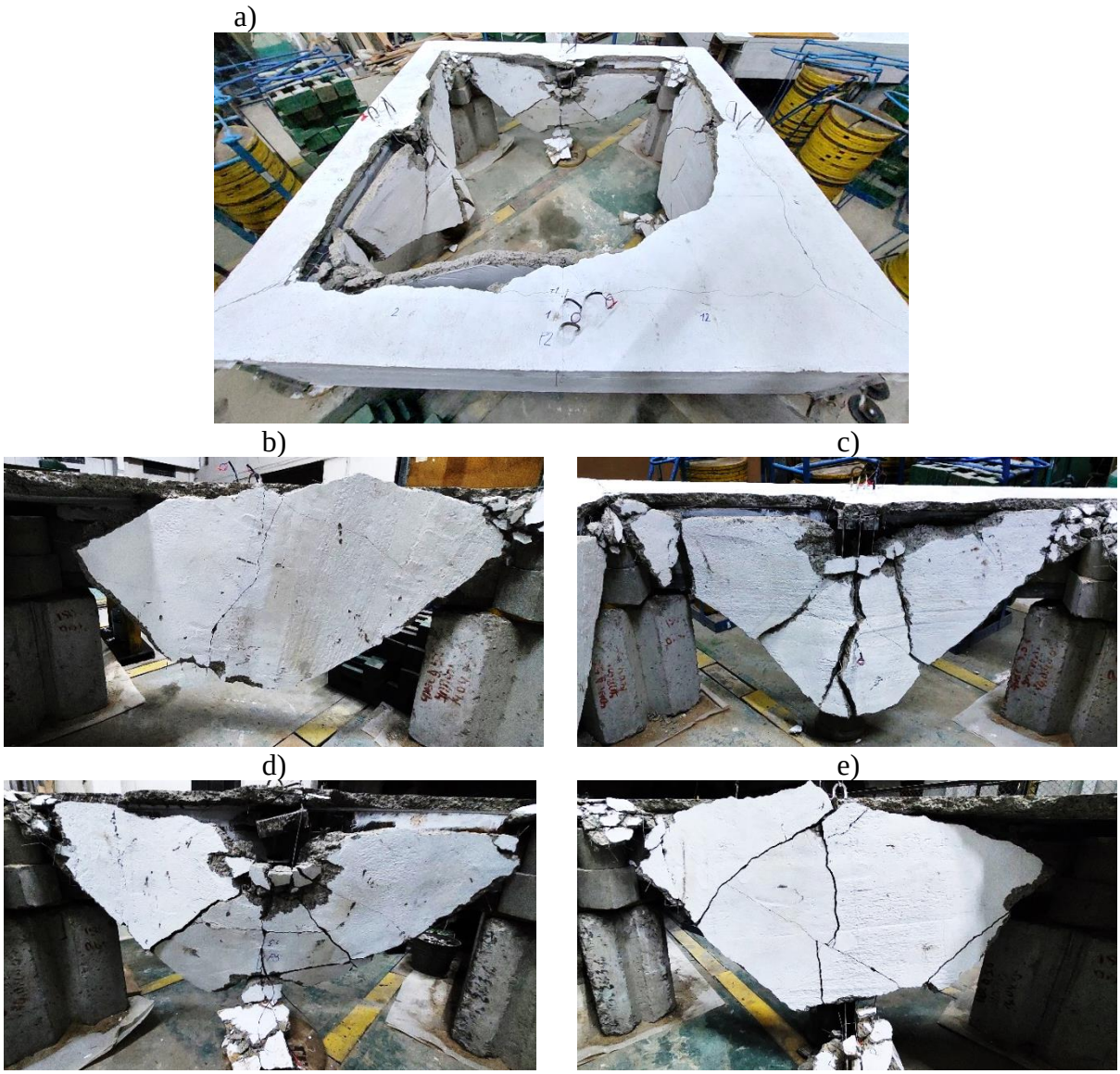

Figure 9. Specimen FS-1 after failure (a); slab segments in the region of column C1 (b); columns C2 (c); columns C3 (d); columns C4 (e)

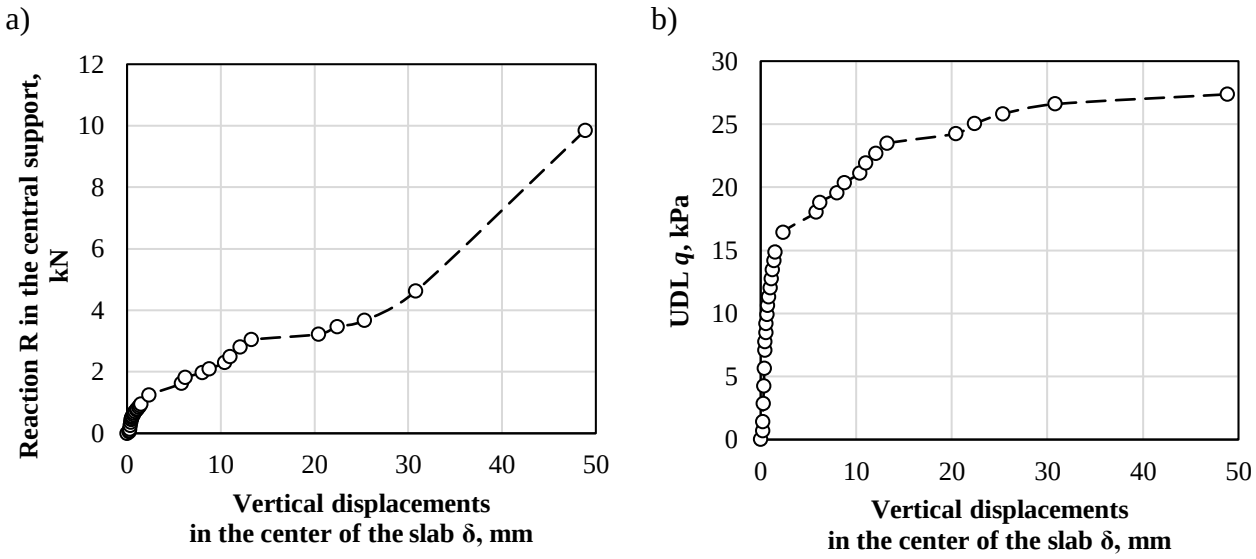

Figure 10. The reaction *R* in the central support (a) and the uniformly distributed load *q* (b) versus the vertical displacements *δ* curves in the center of the span curves

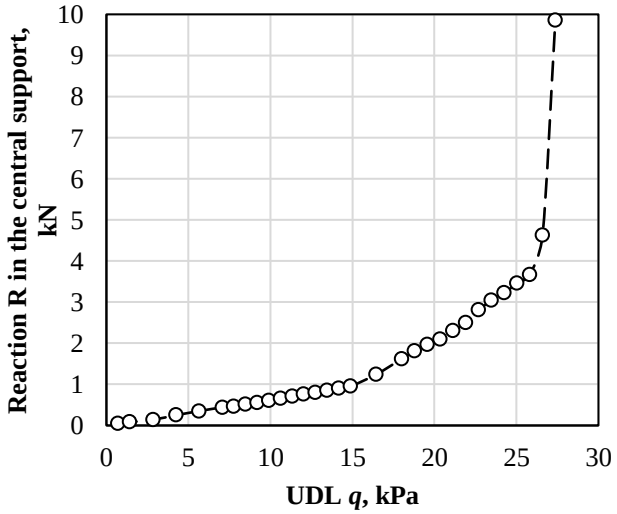

Figure 11. The reaction *R* in the removable support versus the uniformly distributed load *q* curve

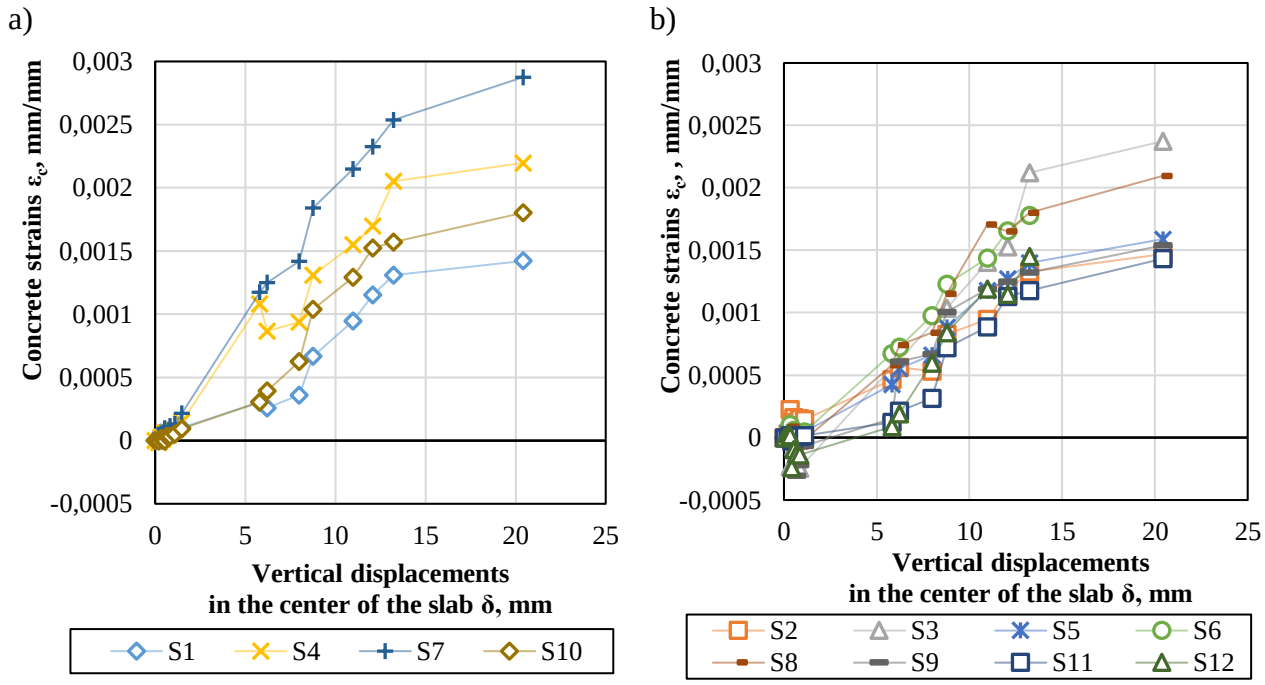

Figure 12. Relationship of the concrete strains ε_c at the top surface of the slab over column (a) and in span (b) versus the vertical displacements δ in the central node

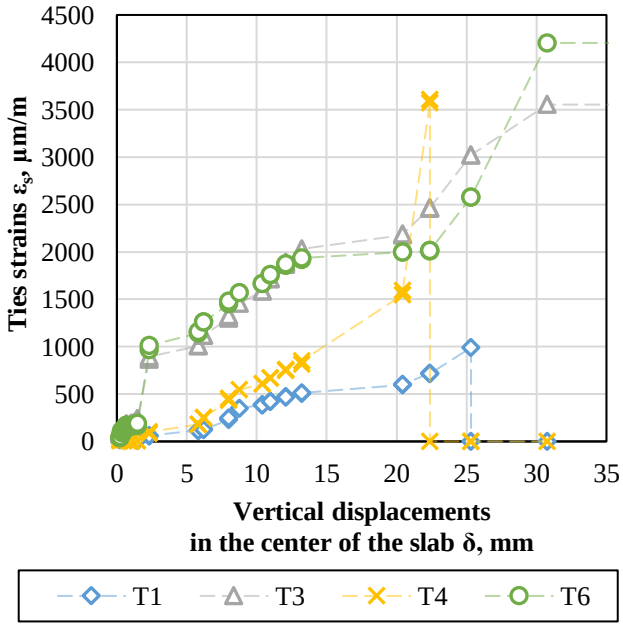

Figure 13. Relationship of the steel ties strains in slab ε_s versus the vertical displacements δ in in the center of the span

During the loading of the FS-1 sample characteristic stages, which correspond to various resistance mechanisms, were observed.

The stage of elastic bending of the slab. Under increasing uniformly distributed load from q = 0 kPa to q = 14.9 kPa the linear increment of vertical displacements δ in the center of the specimen and the reaction in the central support R were observed (corresponding deflections normalized to the effective height of the slab δ/d were increased from 0 to 0.04).

In the area over columns C1-C4, the concrete tensile strains at the top surface (markers S1, S4, S7, S10) and tensile strains of the tie elements (strain gauges T1-T4) corresponding to the elastic bending of the slab were observed. At the same time, concrete strains on markers S4 and S7 (columns C2 and C3) were higher than on markers S1 and S10 (columns C1 and C4). Measurements of the concrete strains at the top of the slab in the span strips (Figure 12b) showed compression in these areas, which may indicate the development of the compressed membrane effect.

The tensile strains of the tie elements had a similar character – the strain registered by the strain gauges T3 (column C3) and T6 (center plate C5) were higher than T1 and T4 (columns C1 and C4).

This development of strains indicates the asymmetry of the work of the sample from the beginning of loading even before the formation of cracks.

The stage of plastic bending of the slab. When uniformly distributed load increase from q = 14.90 kPa to q = 23.47 kPa (δ/d from 0.04 to 0.35) nonlinear behavior (plastic bending) of the slab was observed. The first cracks formed at the top surface of the slab in the area near supports C2 and C3 (along the counter beams B2 and B3) at loads from q = 16.44 kPa to q = 18.01 kPa. At a load of 20.35 kPa, additional cracks formed at the top surface of the slab in the area near supports C1 and C4 (along the counter beams B1 and B4). At the same stage, diagonal cracks were formed at the bottom surface of the slab. These cracks developed from the central support to the corners. Cracks developed at the top surface and diagonal cracks at the bottom surface divided the slab into four segments. In the slab reinforcement (in the bars of the steel wire mesh) the yielding strains were achieved. As load and displacement levels increased, cracks began to concentrate in these regions, signaling the development of a hinge mechanism in the slab. As hinging continued to develop and slab rotation increased in the hinge, the deformation of other slab zones (in area of segments) stabilized and did not significantly increase up to the load level 23.47 kPa.

Internal forces were redistributed in the specimen, as evidenced by a change in the slope of the *R-q* curve (Figure 11).

The strains of the concrete at the top surface in the span strips changed their sign from compression to tension (see Figure 12b), what indicates a disappearance of the compressed membrane effect.

Transition stage. The transition from the flexural slab behaviour to the tensile membrane behaviour for the tested fragment was observed at the load range between q = 23.47 kPa and q = 25.03 kPa (δ/d = 0.35..0.59).

The some reinforcement bars of the slab reached the ultimate tensile strains. This was accompanied by a characteristic sound of wire breaking.

At this stage the plastic rotation of segments in the hinge ensures the achievement of vertical deflections, which are necessary for the development of longitudinal tensile forces in the plane of the slab and the activation of horizontal ties. However, at this stage the contribution from the horizontal ties response to the global resistance of the structural system is insignificant.

The stage of the tensile membrane actions. The tensile membrane forces was developed in tested slab under the load in range from q = 25.03 kPa to 27.37 kPa (δ/d from 0.59 to1.29).

The tensile yield strains of steel in horizontal ties (T3, T4, T6, see Figure 13) were achieved under load q = 25.03 kPa. A new significant redistribution of internal forces was observed in the specimen, as evidenced by a change in the slope of the *R-q* curve (Figure 11).

The membrane actions mostly were taken by the horizontal ties in the column strips of the slab.

The specimen FS1 failure occurred at a load of q = 27.37 kPa (δ/d = 1.29). It was the result of exceeding the ultimate tensile strains in the horizontal ties in the central part of the slab. After breaking of the horizontal ties, the specimen was divided into separate segments along the yield lines (hinges) and collapsed. It is worth noting that the

segments of the slab remained hanging on the tie elements. Cracks along the tie elements on the top face of the slab (Figure 9) are caused by the impact of the segments on the external supports during the collapse.

According to the energy-based method (EBM) the quasi-static response $q(\delta)$ of the FS-1 specimen can be rearranged into a dynamic response $q_d(\delta_d)$ with usage (Eq. 1):

$$q_d(\delta) = \frac{1}{\delta} \cdot \int_0^{\delta} q(\delta) d\delta \qquad (1)$$

Quasi-static response $q(\delta)$ and dynamic response $q_d(\delta)$ according to test results of specimen FS-1 shown in Figure 14.

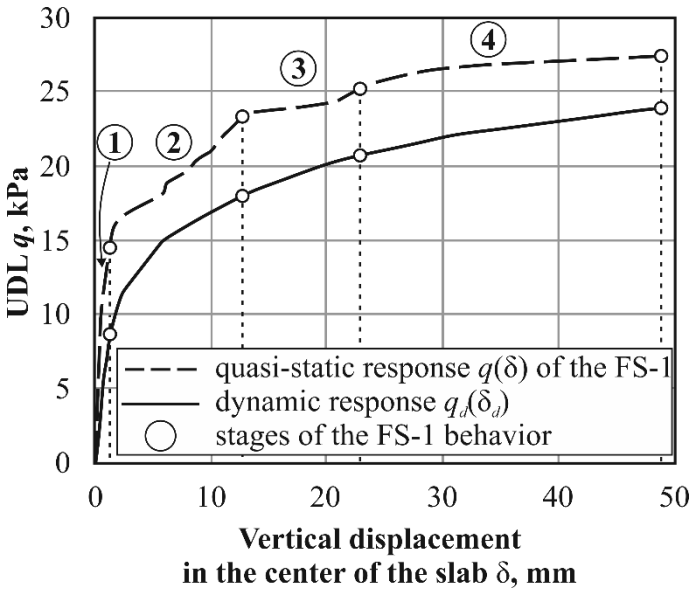

Figure 14. Quasi-static response $q(\delta)$ and dynamic response $q_d(\delta)$ according to test results of specimen FS-1

The basic parameters of the "q-δ" relation, the normalized deflections δ/d, the values of the corresponding dynamic responses and dynamic coefficients are listed in Table 3.

Table 3. Sample FS-1 test results

№	Stages	q, kPa	δ, mm	δ/d, mm/mm	q_d, kPa	k_{qd}	R, kN	R_d, kN
1	elastic bending	14,9	1,49	0,04	8,97	1,66	0,95	0,56
2	plastic bending	23,47	13,23	0,35	18,21	1,29	3,04	1,78
3	transition	25,03	22,39	0,59	20,59	1,22	3,46	2,35
4	tensile membrane	27,37	48,86	1,29	23,87	1,15	9,85	4,43
Note: the dynamic coefficient $k_{qd} = q / q_d$								

As can be seen from Table 3, the value of the dynamic coefficient (k_{qd}) is less than 2.0 (used in linear elastic dynamic calculations) and decreases with increasing load level and deflections. This is due to the dissipation of energy at the half-period of vibration.

2.1 Dynamic test of specimen FS-2

The FS-2 specimen was tested by dynamic load applied to slab after the sudden the central support loss. The following experimental data were obtained:

- pattern of cracking after the sudden loss of the central support (Figure 15)
- the vertical deflections in the center of the slab versus time after sudden support loss, obtained by processing the results of video shooting (figure 16);
- the strains of the ties ε_s versus the time after the sudden support loss (Figure 17).

The crack formation pattern of the FS-2 specimen (Figure 15) practically corresponds to the FS-1 specimen, however, the yield lines (linear hinges) are more symmetrical. When a dynamic load was applied by sudden support loss, the slab was divided into segments by the formed yield lines (plastic hinges).

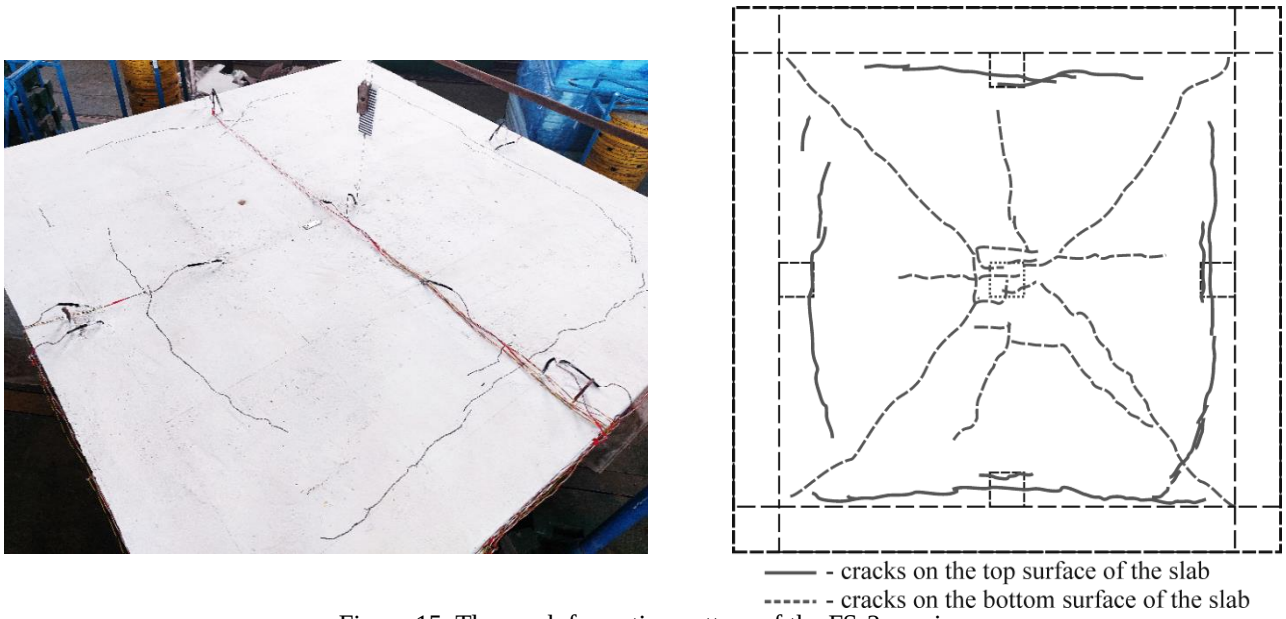

Figure 15. The crack formation pattern of the FS-2 specimen

As can be seen from the "$\delta_d - t$" response (Figure 16), the duration of gravitational load applying of t_g was approximately 100 ms. Such type of loading history corresponds to the case of sudden removal (failure) of a key element [32].

Initial lifting of the slab up before the support loss is due to the mechanism used to removing the support (see Figure 8). In this case, the initial lifting of the slab compensates the deflection from preloading and can be taken as a zero point of reference for vertical deflections after the support loss.

After sudden loss of support, the first half-period of oscillations is the most dangerous for a damaged structural system. According to [19] at this stage the external work of unbalanced loads caused by sudden support loss could be dissipated by the structure if it did not collapse.

As shown in Figure 16, the maximum vertical displacements in the center of the slab were observed during the first half-period of oscillations. Taking into account the initial precamber of the slab, maximum vertical deflection amounted to $\delta_{d,max}$ = 11.7 mm. After that, there were practically no fluctuations and the deflections stabilized at the level of $\delta_{d,s}$ = 11.1 mm. The absence of fluctuations indicates the redistribution of internal forces and the dissipation of energy. From comparison with the experimental data obtained during the testing of the FS-1 specimen, it can be seen that the deflections of the slab $\delta_{d,s}/d$ = 0.31 are in the range of 0.04 to 0.35 corresponding to the stage of plastic bending.

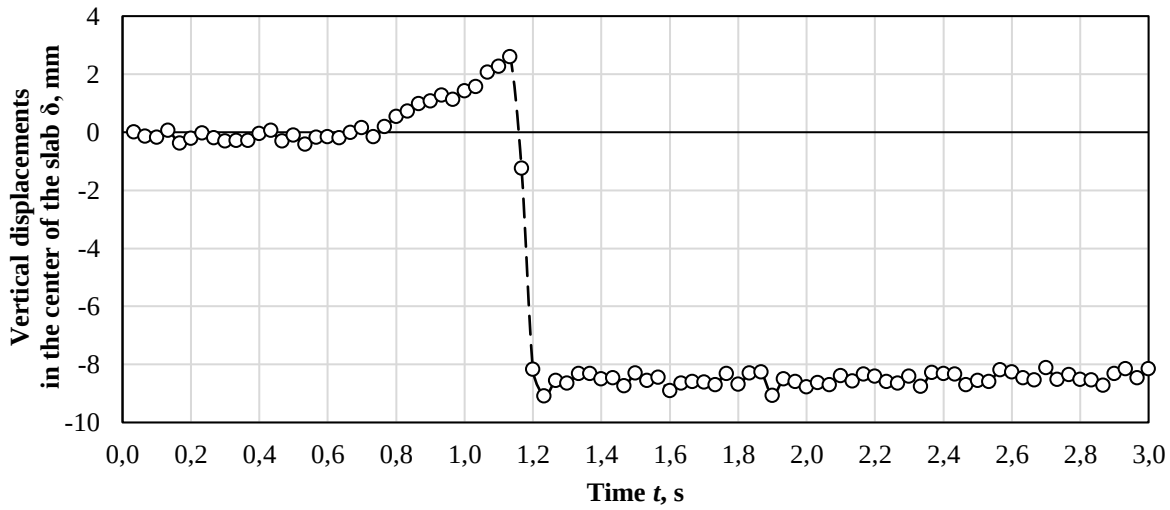

Figure 16. The vertical deflections in the center of the slab FS-2 versus the time after the sudden support loss

From the obtained relation of the strains in the tie elements ε_s versus time (Figure 17), it can be seen that the ties are activated during the time $t_s \approx 1.0$ sec. This time is an order of magnitude longer than the time t_g corresponds the gravitational load applying (the time of the support loss) and the maximum vertical deflections development. The maximum tensile strains in ties were observed in the area of the central column C5. The value of the strain amounted to ε_s = 0.00098 mm/mm and corresponded to the elastic work of the steel ties (see Figure 17).

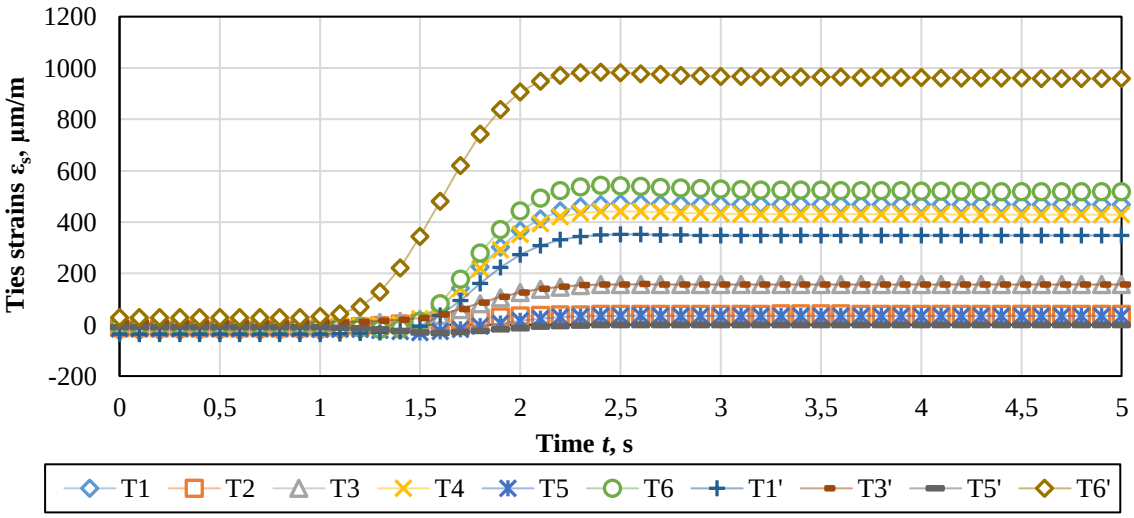

Figure 17. The strains of the ties of the slab FS-2 versus the time after the sudden support loss

3 Conceptual approach to modelling the behaviour of a damaged flat slab with the central support loss

3.1 Principles of macro-modelling

The methods based on the principles of macro-modeling are more promising methods for modeling damaged (modified) structural systems when its robustness checks, than methods based on continuum modeling [37]. According to macro-modeling rules, linear elastic behavior beams and slabs modeled the elastic behavior of the structural system. The nonlinear behavior of the structural systems is modeled by the point plastic hinges. These hinges insert into the certain sections of elements of the structural system according to the accepted rules. Thus, there is a simulation of a discrete-continuum structural system.

Nonlinear plastic hinge in the computational model reflects the local zones in which the plastic rotation and plastic deformations of a real structural system development observed. The places of their into the design scheme should be determined a priori based on a qualitative understanding of the proposed failure mode of the structural system or on the basis of a preliminary analysis performed, for example, using plastic method, based on the provisions of the yield lines theory.

Response of flat slab system(s) after an initial local failure (damage) involves the activation and interaction of several mechanisms in the dynamic domain. Flexural, punching shear, post-punching shear, compressive membrane action and tensile membrane action have been identified as various mechanisms which could influence slab system response. Figure 18 shows an idealized moment-rotation ("*M*-θ"), shear force-rotation ("*V*-ψ") and longitudinal forces-longitudinal displacements ("*N*-*w*") diagrams for main of the listed above mechanisms.

To simplify calculations and reduce the number of plastic hinges types in the calculation model it is possible to use the same type of hinges when modeling plastic bending and shear. In this case, it is necessary to use the "*M*-θ" diagram (Figure 18a) for which the ultimate rotation value is limited in accordance with the punching (post-punching) response of the flat slab (Figure 18b).

The parametric points of the "*N*-*w*" diagram (Figure 18c) should be calculated according to the basic provisions [10, 11].

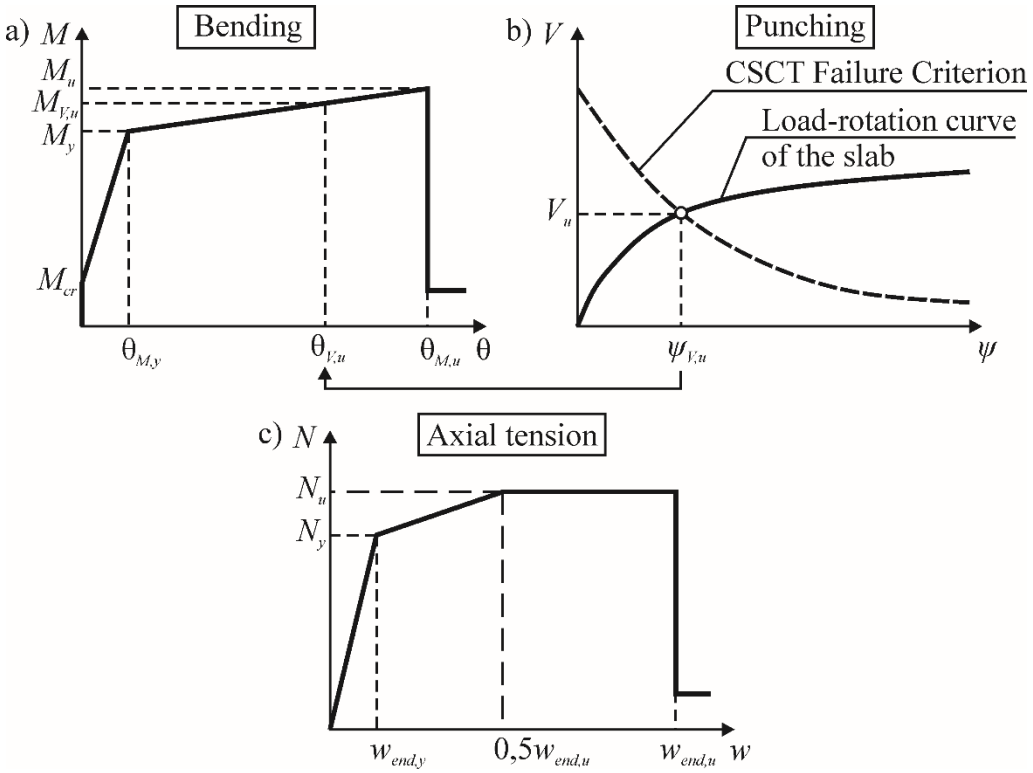

Figure 18. General view of idealized diagrams "*M*-θ" (a), "*V*-θ" (b) and "*N*-*w*" (c)

3.2 Analytical equations for determining the parametric points of a quasi-static «*q*-*δ*» diagram

Stage of elastic behavior

At the stage of the elastic response, the value of deflection δ under uniformly distributed load q can be obtained quite accurately from the solution of the Lagrange equations for thin plates. The solutions of the Lagrange equations for the most common cases of boundary conditions and plate geometry are tabulated by different authors, for example [35].

The load-deflection equation can be represented as follows:

$$\delta = \alpha_1 \frac{q \cdot l^4}{D} \tag{2}$$

where α_1 is the coefficient for determining vertical displacements in the center of the slab ($x = 0$, $y = 0$). In case of square slab clamped along the contour $\alpha_1 = 0.00126$ [35]; D is cylindrical rigidity of the plate without cracks:

$$D = \frac{E_{cm} \cdot h^3}{12\left(1-\upsilon^2\right)} \tag{3}$$

where E_{cm} is the modulus of elasticity of concrete; h is the plate thickness; υ is the Poisson's ratio.

Flexural resistance mechanism.

The flexural mechanism and membrane actions development can be described using analytical equations based on the energy balance method of a modified structural system. For the flexural resistance mechanism describing, the design scheme as illustrated in Figure 19, can be considered.

In accordance with assumption [20], a flat slab is divided by yield lines into segments, which are further considered as a rigid bodies. As can be seen from the own experimental data presented above and from the results of studies obtained by other authors [26, 32, 39], the pattern of cracks formation in flat slabs can be fairly accurately predicted by the yield lines theory.

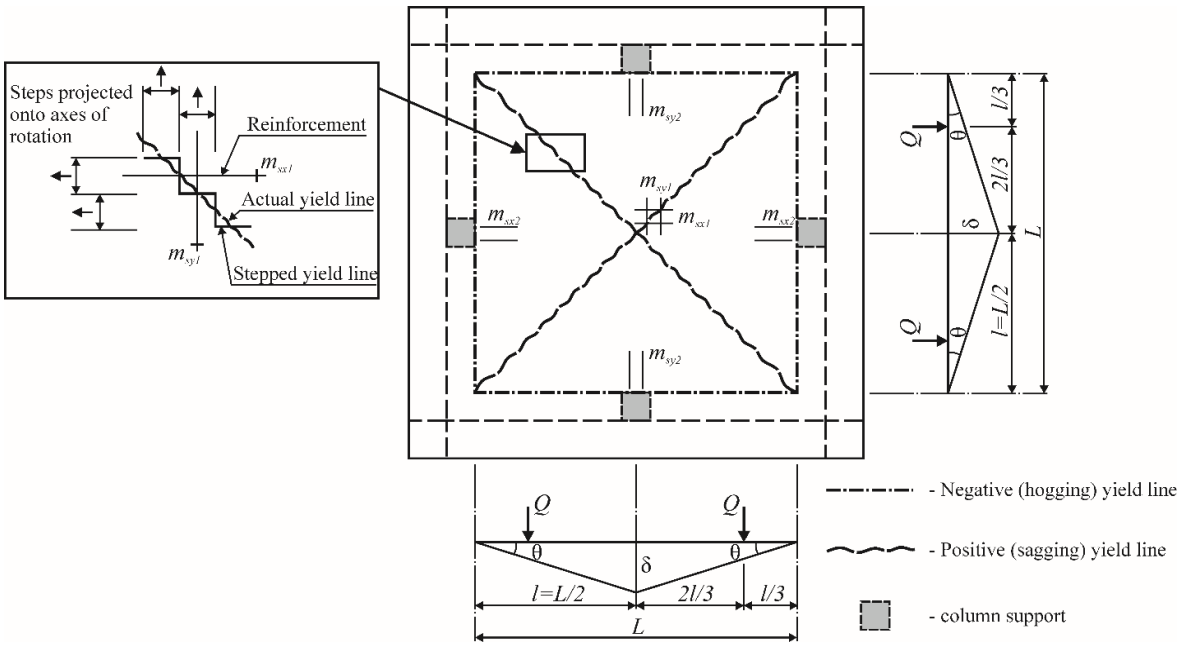

Figure 19. Calculation scheme of sample FS-1 in accordance with the yield lines theory

In accordance with the yield lines theory, a structure is considered at the stage preceding failure, at which the external energy (work) caused by the load on the slab should be equal to the internal energy dissipated within the yield lines:

$$W_{ext} = W_{int} \tag{4}$$

where W_{ext} is the work performed by external gravitational loads Q on the movement displacement δ of the slab segments; W_{int} is the work of the bending moment m_R at the rotation θ.

For an accepted pattern of plastic hinges, the bending moments m acting along the yield lines versus the uniformly distributed load $q(\delta)$, can be expressed in the following simplified form:

$$q(\delta) = \frac{24 \cdot \left(m_1(\delta) + m_2(\delta) \right)}{L^2} \tag{5}$$

The values of the bending moments m are determined from the diagrams "M-θ" (see Figure 19) with the limitation of the ultimate moment accounting the punching resistance of the slab in an accidental design situation.

Shear resistance of the slab

To estimate the punching shear resistance, a model based on the critical shear crack theory (CSCT) can be used [12, 23, 24].

In [23], the following modified equations of the failure criterion are proposed for different strain rates:

$$\frac{V_R}{b_0 d_V \sqrt{f_c}} = \frac{0.8}{1+\frac{15\psi d}{d_{g0}+d_g}} \text{ for } \dot{\varepsilon} = 10/s$$
$$\frac{V_R}{b_0 d_V \sqrt{f_c}} = \frac{1}{1+\frac{15\psi d}{d_{g0}+d_g}} \text{ for } \dot{\varepsilon} = 100/s \quad (6)$$
$$\frac{V_R}{b_0 d_V \sqrt{f_c}} = \frac{1.3}{1+\frac{15\psi d}{d_{g0}+d_g}} \text{ for } \dot{\varepsilon} = 300/s$$

According to equations (6), at low strain rates, insignificant increments of shear resistance are observed. In general case the shear resistance increases with increasing of the strain rates.

In accordance with ***fib***Model Code 2010 [12, 24], for 2-level approximation, the shear force is determined for the rotation calculated by following expression:

$$\psi = \frac{3}{2} \cdot \frac{r_s}{d} \cdot \frac{f_y}{E_s} \cdot \left(\frac{M_{sd}}{M_{Rd}} \right)^{3/2} \quad (7)$$

where r_s is the position of zero radial bending moment relative to the support axis (usually taken equal to $0.22L$ for flat slabs with a span L), E_s is the modulus of elasticity of steel reinforcement, M_{sd} is the average bending moment per unit length in the column strip (in the support area) of the slab, and M_{Rd} is the average bending strength per unit length in the column strip.

For the case of internal columns according to ***fib***Model Code 2010 [12], M_{sd} is related to the load V_d as follows:

$$M_{sd} = \frac{V_d}{8} \quad (8)$$

Tensile membrane mechanism

After the yield lines formation and the sufficient plastic rotation development in the hinges the tie elements are activated at the post-punching stage (Figure 20).

The resultant of the tie forces in the design scheme (Figure 20) can be considered as the response of the system, balancing the gravitational force *Q* acting in its center of mass. In this case, resistance can be defined as quasi-static or dynamic. Within the framework of the energy approach [37], the static resistance depends on the amount of displacement and can be described by the resistance function $q_{stat}\ (\delta_{qz})$, which depends on the "*N*-*w*" diagram for plastic axial hinges in the slab (see Figure 18c).

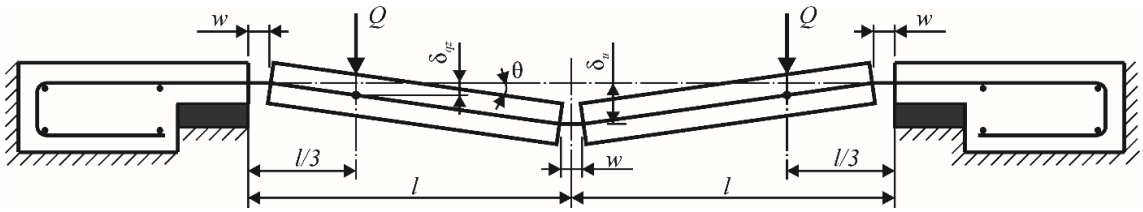

Figure 20. Design scheme of a flat slab to determine the membrane effect at large displacements

If all ties elements of the damaged system are of the same type, then they have the same "*N*-*w*" relationship. Self-weight and other permanent loads are represented by the net force *Q* applied at its center of mass. The deformed state is determined by the vertical displacement δ_{qz} (see Figure 20).

For identical horizontal displacements w of all bonded joints, the vertical displacement δ_{qz} can be calculated directly from the geometry of the deformed scheme as (see Figure 20):

$$\delta_{qz} \approx \frac{\sqrt{3 \cdot l \cdot w}}{3} \tag{9}$$

where *l* is the segment length.

Then the maximum vertical displacement in the center of the slab:

$$\delta_u = 3 \cdot a_{qz} = \sqrt{3 \cdot l \cdot w_u} \tag{10}$$

Energy balance conditions for a system consisting of four segments and having horizontal ties in the above-column strips in two directions:

$$Q \cdot a_{qz,u} = \frac{3}{2} \cdot \xi(w_u) \cdot N_u \cdot w_u \tag{11}$$

where $\xi(w_u)$ is the relative strain energy of the bond according to ***fib*** Bulletin 43[ ]:

$$\xi(w) = \frac{\int_0^w N(w)dw}{N_u \cdot w} \tag{12}$$

It is obvious from Eq. (11) that the resistance of the chain system depends not only on the tensile strength *N* of the ties, but also on their plastic deformability w, i.e. elongation ability.

For a laterally restrained slab, the value of vertical deflections δ_t, corresponding to the activation of membrane effects, can be taken a priori as 0.5*d* or more. From the analysis of the test results for sample FS-1, it follows that the onset of a pronounced influence of the effects of the tensile membrane corresponds to the vertical deflections approximately equal to 0.59*d*. For example, in [39], for a slab specimen in which there were no rigid horizontal restraint along the contour, this parameter was equal to 0.87*d*.

3.3 Calculation of prototypes FS-1 and FS-2

At the first stage, to describe the flexure failure mechanism with limitation of the ultimate hinge rotation based on the punching shear failure criterion the idealized "*M*-φ" diagram (see Figures 18a and 18b) and "*N*-*w*" relation which describes the mechanism of membrane forces (see Figure 18c) for specimens FS-1 and FS-2 were determined. The mechanical properties of materials which were used for evaluation of the parametric points of diagrams "*M*-θ" and "*N*-*w*" are given in Tables 1 and 2.

The bending plastic hinge is described by the "*M*-θ" relation, which is obtained on the basis of the relation "M-φ" for the critical sections on the supports and in the middle of the span of the slab. The width of the critical sections was taken as equal to b = 1.7 m (as the length of the projection of the yield lines on the axis of rotation of an individual segment). The length of the flexure plastic hinge in the first approximation was taken as equal to the effective depth of the section d (based on the characteristic pattern of cracking obtained in the experiments).

The moments M_y and M_u, corresponding to yielding in the tensile reinforcement and the achievement of ultimate compressive strains of concrete, respectively, as well as the corresponding curvature values φ_y and φ_u, were obtained from the sections design.

The parametric points of the moment-curvature relationship "*M*-φ" are presented in Table 4.

Table 4. The parametric points of the "*M*-*φ*" relationship for FS-1 and FS-2 specimens

Specimen	**Section**	**Bending moment**		**Curvature**	
		M_y **N·mm per 1,7 m**	M_u **N·mm per 1,7 m**	φ_y **1/mm**	φ_u **1/mm**
FS-1	span	1,74E+06	2,11E+06	1,54E-04	3,14E-03
	support	0,99E+06	1,27E+06	2,05E-04	3,27E-03
FS-2	span	1,76E+06	2,14E+06	1,67E-04	3,42E-03
	support	1,01E+06	1,29E+06	2,08E-04	3,56E-03
Note: the general view of the "*M*-φ" diagram corresponds to the "*M*-θ" diagram, see Figure 18a.					

Axial plastic hinges model membrane effects and are described using "*N*-*w*" diagrams, the parametric points of which are obtained in accordance with [10, 11] and are given in Table 5.

Table 5. The parametric points of the "N-w" diagram for FS-1 and FS-2 specimens

Ties	**Longitudinal forces**		**Longitudinal displacements**		
	N_y**, kN**	N_u**, kN**	$w_{end,y}$**, mm**	**0,5**$w_{end,u}$**, mm**	$w_{end,u}$**, mm**
3Ø4	22,41	26,27	0,17	0,86	1,71
Note: the general view of the "*N*-*w*" diagram, see Figure 18c.					

At the second stage the parameters defining the mean "*q*-*δ*" relationships for samples FS-1 and FS-2 were performed according to the equations proposed above (see Eq. (2) – (12)). Also, for comparison, a nonlinear quasi-static analysis of the FS-1 specimen and a nonlinear dynamic analysis of the FS-2 specimen were performed with usage software SAP2000. Moreover, the FEM-analysis performed by SAP2000 took into account the geometric non-linearity (second order effects) of the system.

To modeling of the flat slabs, a frame approximation was used. The mean parameters defining the plastic hinge relationships which were used in analysis are presented in Tables 5 and 6. When a nonlinear dynamic analysis of the sample FS-2 was performed using SAP2000, a fixed value of the damping coefficient was taken as equal to 3.5%.

The results of analysis for samples FS-1 and FS-2 obtained based on analytical equations (1) – (12) and with using SAP2000 are shown in Figure 21 and Figure 22 and in Table 6.

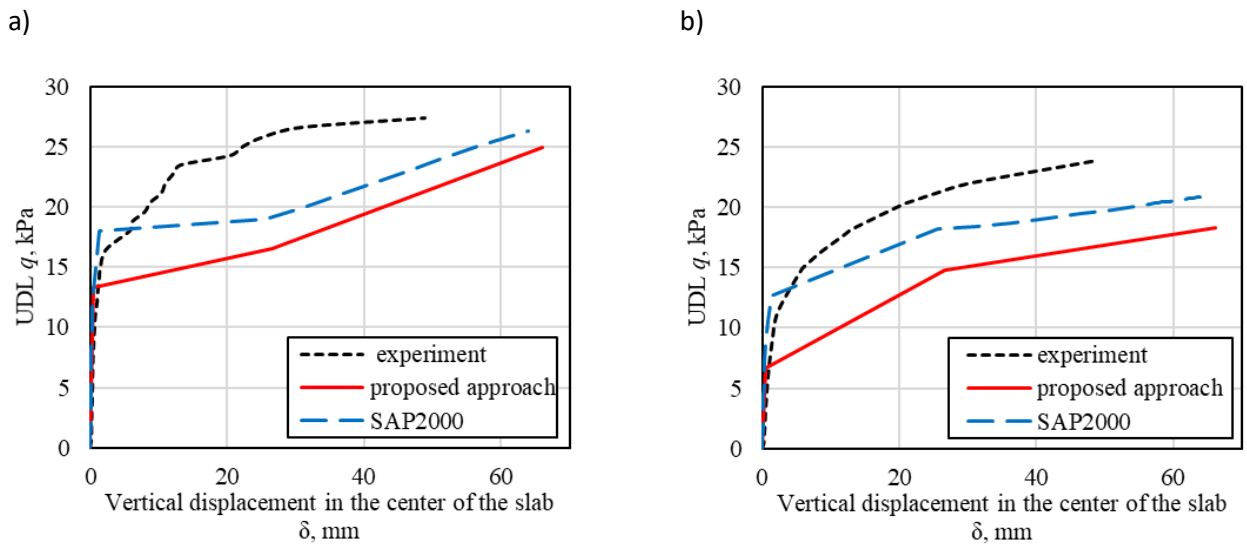

Figure 21. *The results of analyses for sample FS-1 (a) quasi-static response "q-δ";*
(b) dynamic response "q_d-δ"

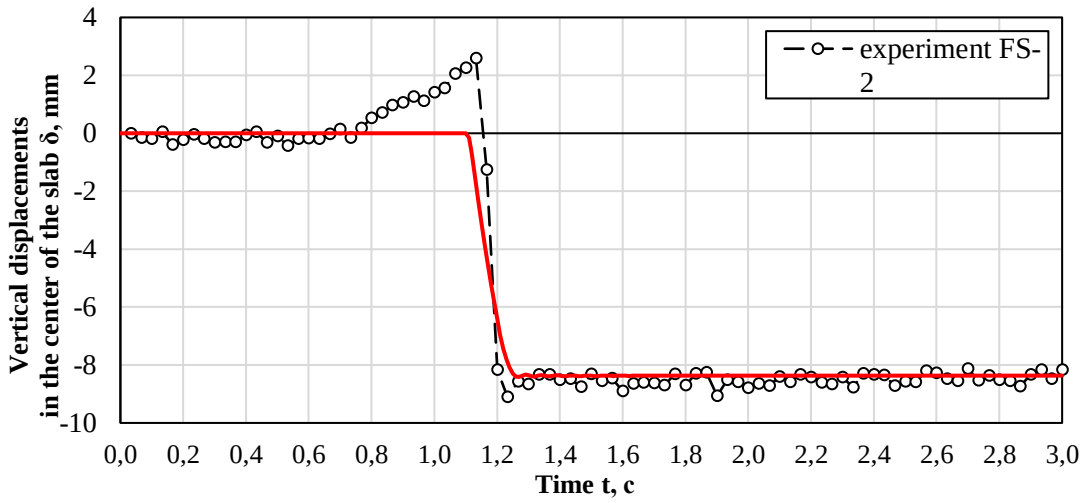

Figure 22. – *Results of nonlinear dynamic analysis of slab FS-2*

Table 6. The results of analysis for samples FS-1 and FS-2

Stages	Parameter	Unit	FS-1			FS-2	
			Exp.	Theor.	SAP2000	Exp.	SAP2000
Elastic bending	δ_y,	mm	1.49	0.55	1.10	-	-
	q_y,	kN/m^2	14.9	13.34	17.0	-	-
Plastic bending	δ_t,	mm	22.39	26.55	25.62	11.70	8.37
	q_u,	kN/m^2	25.03	16.51	19.00	20.24	20.24
Tensile membrane	δ_u,	mm	48.86	66.10	63.96	-	-
	q_{u2},	kN/m^2	27.37	24.99	26.3	-	-
	q_{du} (dyn. resp.)	kN/m^2	23.87	18.34	20.88	-	-

As can be seen from the presented results of a comparative analyses, the calculated quasi-static diagrams obtained based on proposed analytical equations (2) – (12) differ from the experimental ones. This can be explained by the different type of loading mode. In the experiment, there was a loading mode with load control. In the numerical analyses, diagrams corresponding to the loading mode with displacement control were obtained. Also, the proposed analytical equations did not take into account the effects of a compressed membrane, which leads to a more conservative solution.

4 Conclusions

The presented experimental studies allow us to draw the following conclusions:

1. In structural systems with flat slabs, in an accidental design situation, various mechanisms of resistance to progressive collapse arise. A correct understanding of their origin and development allows more rational and safe design of structures that will meet the requirements of robustness in accidental design situations.

2. Tests of the FS-1 specimen performed by the static unloading method made it possible to identify and study in detail the characteristic stages of the behavior of a flat slab when removing a vertical load-bearing element. As a result, a complete nonlinear quasi-static response of the structural system is obtained.

3. Dynamic tests of the FS-2 specimen allowed us to establish that various resistance mechanisms are not activated simultaneously during sudden dynamic application of the load, which affects the instantaneous dynamic response of the system. For the loading level corresponding to the stage of plastic bending, there was a redistribution of internal forces and the activation of tie elements after the realization of maximum deflections at the first half-period of oscillations.

4. Against the background of experimental data, computational dependencies were examined to determine the parameters defining a quasi-static response diagram of a damaged structural system in an accidental design situation. In the long term, taking into account the modeling error, these dependencies may allow parametric studies and statistical calibrations of safety coefficients to check the robustness of structural systems.

5. It is established that the tie elements in the above-column areas allow to perceive membrane forces, and also increase the shear resistance of the slab around the columns adjacent to the remote one.

References

1. Adam, J. M., Parisi, F., Sagaseta, J., and Lu, X. (2018). Research and practice on progressive collapse and robustness of building structures in the 21st century. *Engineering Structures*, *173*, 122-149. DOI: 10.1016/j.engstruct.2018.06.082.
2. ASCE. (2005). Minimum design loads for buildings and other structures. American Society of Civil Engineers.
3. British Standard BS 8110-11. (1997). The structural use of concrete in building – Part 1: Code of practice for design and construction. London, U.K.
4. Chen, Z., Zhu, Y., Lu, X., and Lin, K. (2023). A simplified method for quantifying the progressive collapse fragility of multi-story RC frames in China. *Engineering Failure Analysis*, *143*, DOI: 10.1016/j.engfailanal.2022.106924.

5. Dat, P. X., and Tan, K. H. (2013). Experimental study of beam–slab substructures subjected to a penultimate-internal column loss. *Engineering Structures, 55*, 2-15. DOI: 10.1016/j.engstruct.2013.03.026.
6. Dat, P. X., and Tan, K. H. (2015). Experimental response of beam-slab substructures subject to penultimate-external column removal. *Journal of Structural Engineering, 141*(7), 1-12. DOI: 10.1061/(ASCE)ST.1943-541X.0001123.
7. DoD UFC Guidelines. (2005). Design of Buildings to Resist Progressive Collapse, Unified Facilities Criteria (UFC) 4-023-03. Department of Defense (DoD).
8. Ellingwood, B. R., Smilowitz, R., Dusenberry, D. O., Duthinh, D., Lew, H. S., & Carino, N. J. (2007). Best practices for reducing the potential for progressive collapse in buildings. NISTIR 7396. National Institute of Science and Technology, US Deparment of Commerce.
9. European Committee for Standardization. (2006). Eurocode 1 - EN 1991-1-7: Actions on structures - Part 1-7: General actions - Accidental actions.
10. ***fib*** Bulletin 43: Structural connections for precast concrete buildings. Guide to good practice. 2008.
11. ***fib*** Bulletin 72. Bond and anchorage of embedded reinforcement: Background to the fib Model Code for Concrete Structures 2010: Technical report. *fib*-Fédération internationale du béton, 2014; 72.
12. ***fib*** Model Code for Concrete Structures 2010. (2010). International Federation for Structural Concrete (*fib*), Lausanne, Switzerland.
13. General Service Administration (GSA). (2003.). Progressive collapse analysis and design guidelines for new federal office buildings and major modernization projects. Washington (DC).
14. GOST 10180-2012 (2015). Concretes. Methods for strength determination using reference specimens. Minsk. (In Russian).
15. GOST 12004-81 (2011). Reinforcing-bar steel. Tensile test methods. (In Russian).
16. GOST 24452-80. Concretes. Methods of prismatic, compressive strength, modulus of elasticity and Poisson's ratio determination. (In Russian).
17. Herraiz B., Vogel T. and Russell J. (2015). Energy-based method for sudden column failure scenarios: theoretical, numerical and experimental analysis. In *IABSE Workshop Helsinki 2015: Safety, Robustness and Condition Assessment of Structures. Report* (pp. 70-77). International Association for Bridge and Structural Engineering IABSE. DOI: https://doi.org/10.3929/ethz-a-010389549.
18. International Standard Organization. (2015). ISO 2394: General principles on reliability for structures, Fourth ed. Genève, Switzerland.
19. Izzuddin, B. A., Vlassis, A. G., Elghazouli, A. Y., & Nethercot, D. A. (2008). Progressive collapse of multi-storey buildings due to sudden column loss—Part I: Simplified assessment framework. *Engineering structures, 30*(5), 1308-1318. DOI: 10.1016/j.engstruct.2007.07.011.
20. Kennedy, G., & Goodchild, C. H. (2004). Practical yield line design. *Concrete Centre, Surrey, UK*.
21. Lim, N. S., Tan, K. H., and Lee, C. K. (2017). Experimental studies of 3D RC substructures under exterior and corner column removal scenarios. *Engineering Structures, 150*, 409-427. DOI: 10.1016/j.engstruct.2017.07.041.

22. Ma, F., Gilbert, B. P., Guan, H., Xue, H., Lu, X., and Li, Y. (2019). Experimental study on the progressive collapse behaviour of RC flat plate substructures subjected to corner column removal scenarios. *Engineering Structures, 180*, 728-741. DOI: 10.1016/j.engstruct.2018.11.043.
23. Micallef, K., Sagaseta, J., Ruiz, M. F., and Muttoni, A. (2014). Assessing punching shear failure in reinforced concrete flat slabs subjected to localised impact loading. *International Journal of Impact Engineering, 71*, 17-33. DOI: 10.1016/j.ijimpeng.2014.04.003.
24. Muttoni, A. (2008). Punching shear strength of reinforced concrete slabs without transverse reinforcement. *ACI structural Journal, 105*, 440-450. DOI: 10.14359/19858.
25. Pang, B., Wang, F., Yang, J., Nyunn, S., & Azim, I. (2021). Performance of slabs in reinforced concrete structures to resist progressive collapse. In *Structures* (Vol. 33, pp. 4843-4856). Elsevier. DOI: 10.1016/j.istruc.2021.04.092.
26. Pham, A. T., Lim, N. S., and Tan, K. H. (2017). Investigations of tensile membrane action in beam-slab systems under progressive collapse subject to different loading configurations and boundary conditions. *Engineering Structures, 150*, 520-536. DOI: 10.1016/j.engstruct.2017.07.060.
27. Preece, B. W., and Davis, D. D. (1974). Modeling of reinforced concrete structures. Minsk: The highest school. (In Russian).
28. Qian, K., and Li, B. (2012). Slab effects on response of reinforced concrete substructures after loss of corner column. *ACI Structural Journal, 109*(6), 845-855.
29. Qian, K., Li, B., and Ma, J. X. (2015). Load-carrying mechanism to resist progressive collapse of RC buildings. *J. Struct. Eng, 141*(2), 1-14. DOI: 10.1061/(ASCE)ST.1943-541X.0001046.
30. Qian, K., and Li, B. (2015). Research advances in design of structures to resist progressive collapse. *Journal of Performance of Constructed Facilities, 29*(5), B4014007. DOI: 10.1061/(ASCE)CF.1943-5509.0000698.
31. Ren, P., Li, Y., Lu, X., Guan, H., and Zhou, Y. (2016). Experimental investigation of progressive collapse resistance of one-way reinforced concrete beam–slab substructures under a middle-column-removal scenario. *Engineering Structures, 118*, 28-40. DOI: 10.1016/j.engstruct.2016.03.051.
32. Russell, J. M., Owen, J. S., and Hajirasouliha, I. (2015). Experimental investigation on the dynamic response of RC flat slabs after a sudden column loss. *Engineering Structures, 99*, 28-41. DOI: 10.1016/j.engstruct.2015.04.040.
33. SN 2.01.01-2019. (2020). Basics of design of building structures. Minsk. (In Russian).
34. SP 5.03.01-2020. (2020). Concrete and reinforced concrete structures. Minsk. (In Russian).
35. Timoshenko S., Woinowsky-Krieger S. (1987). Theory of Plates and Shells, 2nd ed. New York City, United States of America: McGraw-Hill.
36. Tohidi, M. (2015). Effect of floor-to-floor joint design on the robustness of precast concrete cross wall buildings (Doctoral dissertation, University of Birmingham).
37. Tur, V., Tur, A., and Lizahub, A. (2021). Simplified analytical method for the robustness assessment of precast reinforced concrete structural systems. *Budownictwo i Architektura, 20*(4), 93-114. DOI: 10.35784/bud-arch.2774.

38. Wieczorek, M. (2013). Influence of amount and arrangement of reinforcement on the mechanism of destruction of the corner part of a slab-column structure. *Procedia Engineering, 57*, 1260-1268. DOI: 10.1016/j.proeng.2013.04.159.
39. Yi, W. J., Zhang, F. Z., and Kunnath, S. K. (2014). Progressive collapse performance of RC flat plate frame structures. *Journal of Structural Engineering, 140*(9), 1-10. DOI: 10.1061/(ASCE)ST.1943-541X.0000963.
40. Chmielewski R., Baryłka A., Obolewicz J. *The impact of design and executive errors affecting the damage to the floor of the concert hall.* Journal of Achievements in Materials and Manufacturing Engineering 2021; 2 (104): (str. 49-56) doi 10.5604/01.3001.0014.8488